Regulation and Function of the Interleukin 13 Receptor α 2 During a T Helper Cell Type 2–dominant Immune Response

Monica G. Chiaramonte,[1] Margaret Mentink-Kane,[1]
Bruce A. Jacobson,[2] Allen W. Cheever,[3] Matthew J. Whitters,[2]
Mary E.P. Goad,[2] Anthony Wong,[2] Mary Collins,[2]
Debra D. Donaldson,[2] Michael J. Grusby,[4] and Thomas A. Wynn[1]

[1]*Immunopathogenesis Section, Laboratory of Parasitic Diseases, National Institute of Allergy and Infectious Diseases, National Institutes of Health (NIH), Bethesda, MD 20892*
[2]*Wyeth-Genetics Institute, Cambridge, MA 01810*
[3]*Biomedical Research Institute, Rockville, MD 20852*
[4]*Department of Immunology and Infectious Diseases, Harvard School of Public Health, Boston, MA 02115*

The Journal of Experimental Medicine

Abstract

Highly polarized type 2 cytokine responses can be harmful and even lethal to the host if they are too vigorous or persist too long. Therefore, it is important to elucidate the mechanisms that down-regulate these reactions. Interleukin (IL)-13 has emerged as a central mediator of T helper cell (Th)2-dominant immune responses, exhibiting a diverse array of functional activities including regulation of airway hyperreactivity, resistance to nematode parasites, and tissue remodeling and fibrosis. Here, we show that IL-13 receptor (R)α2 is a critical down-regulatory factor of IL-13–mediated tissue fibrosis induced by the parasitic helminth *Schistosoma mansoni*. IL-13Rα2 expression was induced after the onset of the fibrotic response, IL-10, IL-13, and Stat6 dependent, and inhibited by the Th1-inducing adjuvant IL-12. Strikingly, schistosome-infected C57BL/6 and BALB/c IL-13Rα2–deficient mice showed a marked exacerbation in hepatic fibrosis, despite displaying no change in granuloma size, tissue eosinophilia, or mastocytosis. Fibrosis increased despite the fact that IL-13 levels decreased significantly in the liver and serum. Importantly, pathology was prevented when IL-13Rα2–deficient mice were treated with a soluble IL-13Rα2-Fc construct, formally demonstrating that their exacerbated fibrotic response was due to heightened IL-13 activity. Together, these studies illustrate the central role played by the IL-13Rα2 in the down-regulation of a chronic and pathogenic Th2-mediated immune response.

Key words: fibrosis • inflammation • liver • granuloma • mouse

Introduction

Type 2 cytokines including IL-4, IL-10, and IL-13 are often described as antiinflammatory mediators because they inhibit type 1–dominated cell-mediated immune responses (1). Nevertheless, studies of allergy, asthma, and the response to extracellular helminths clearly demonstrate that many type 2 cytokines can also act as proinflammatory mediators (2). Indeed, several recent studies have demonstrated that highly polarized immune responses may become detrimental or even lethal to the host if they are too vigorous or become chronic, regardless of whether type 1 or type 2 cytokines dominate the response (3–5). In each case, however, distinct forms of immune-mediated pathology develop as a consequence of sustained cytokine production (6, 7). Therefore, understanding the various control mechanisms that suppress or inhibit chronic inflammatory reactions is of utmost importance.

In schistosomiasis, a chronic inflammatory disease of the liver and gut, Th2 cytokines are required for normal granuloma formation and development of hepatic fibrosis (8). Indeed, several studies have shown that type 1 cytokines re-

M.G. Chiaramonte and M. Mentink-Kane contributed equally to this work.

Address correspondence to Thomas A. Wynn, Immunopathogenesis Section, Laboratory of Parasitic Diseases, National Institute of Allergy and Infectious Diseases, National Institutes of Health, Building 50, Room 6154, MSC 8003, Bethesda, MD 20892. Phone: 301-496-4758; Fax: 301-480-5025; E-mail: twynn@niaid.nih.gov

M.G. Chiaramonte's present address is Division of Immunobiology, The Children's Hospital Research Foundation, 3333 Burnet Avenue, Cincinnati, OH 45229.

duce fibrotic pathology whereas Th2 cytokines play critical roles in the pathogenesis of the disease (5, 9–12). Development of the Th2 response is highly dependent upon IL-4 and IL-4 receptor expression (13, 14) whereas IL-10 appears to act as a potent immunosuppressive cytokine, reducing both type 2 cytokine production and granulomatous inflammation (5, 15). Notably, however, recent studies suggested an even more critical role for IL-13, revealing it as the key mediator of the fibrotic response (11, 12), the primary cause of morbidity and mortality in human schistosomiasis (16). IL-13 is highly abundant during schistosome infection and is produced at levels far exceeding IL-4, approaching 100-fold more (11). Thus, although both cytokines utilize the IL-4Rα chain for signaling and exhibit similar functional activities, IL-13 plays a more important role in the pathogenesis of fibrosis. Consistent with this conclusion, studies conducted in related models also demonstrated critical roles for IL-13 in resistance to gastrointestinal nematode infection (17–19), tumor immunosurveillance (20), and in the pathogenesis of asthma (21–23). Therefore, a better understanding of the mechanisms that control the production and/or activity of IL-13 in vivo is particularly important.

Many similarities and differences in function between IL-4 and IL-13 might be explained by the organization of the receptor complex that binds these cytokines. The most accepted model for the IL-4–IL-13 receptor complex suggests there are at least three different receptor combinations. The type I receptor is composed of the common IL-2Rγ chain (γc; reference 24) and the unique IL-4Rα chain, with the latter serving as the signaling receptor. There is also a type II IL-4R, which is composed of the IL-4Rα and IL-13Rα1 chains (25, 26). The type I receptor, found mainly on hematopoietic cells, binds only IL-4 whereas the type II receptor interacts with IL-4 and IL-13 with high affinity and is found primarily on nonhematopoietic cells (26, 27). Recently, a second IL-13R chain, IL-13Rα2 (28), was cloned and characterized in mice (29). This third receptor can also exist as a soluble receptor and binds IL-13 exclusively with much higher affinity than the IL-13Rα1 chain. Structural differences between the cytoplasmic domains of the IL-13 receptors suggest they are functionally distinct, raising the possibility that IL-13Rα2 is a dominant-negative inhibitor or a decoy receptor for IL-13 (29–32). The absence of signaling activity combined with high ligand affinity and high expression levels on cells such as fibroblasts (33), match the criteria for a decoy receptor, as originally described for the decoy IL-1R type II (34). Interestingly, this receptor was recently engineered as a soluble IL-13Rα2-Fc (sIL-13Rα2-Fc)* fusion protein and has been used successfully to block several functions attributed to IL-13, including fibrogenesis (11), airways hyperreactivity (22, 23, 35, 36), and gastrointestinal parasite expulsion (19, 37). Nevertheless, no previous studies have examined the regulation or function of the endogenous IL-13Rα2 in an important Th2-dependent disease model.

In this study, we investigate the regulation and function of the IL-13Rα2 in mice infected with *Schistosoma mansoni*. In initial studies, we examined whether IL-4/IL-13 receptor expression is modulated in the liver after infection. Additional studies were conducted in various KO mice to determine whether type 1/type 2 cytokines regulate IL-13Rα2 mRNA and protein expression in vivo. Finally, mice with targeted deletion of the IL-13Rα2 (38) were infected with the parasite to determine whether the endogenous IL-13Rα2 exhibits either inhibitory or stimulatory activities during a chronic Th2-dominant immune response. Our results show that IL-4Rα and IL-13Rα2 are differentially regulated in the liver during the course of *S. mansoni* infection. Moreover, we show that IL-13Rα2 is regulated by its own ligand, IL-13. Finally, and perhaps of most importance, we show that IL-13–dependent liver fibrosis increases dramatically in the absence of the IL-13Rα2, despite the fact that local Th2 cytokine production is simultaneously decreased. As such, these results reveal an important decoy function for the IL-13Rα2 and illustrate how IL-13 receptor expression may significantly alter the development of type 2 cytokine-dependent pathology.

Materials and Methods

Animals, Parasite Infections, and Antigen Preparations. 6–8-wk-old female C57BL/6, BALB/c, and C3H/HeN mice were obtained from the Division of Cancer Treatment, National Cancer Institute. IL-4, IL-4/IL-10, IL-10, IL-12, IL-10/IL-12–deficient, and WT C57BL/6 mice were generated as previously described (39) and obtained from Taconic Farms Inc. Breeding pairs of IL-13–deficient and WT mice were provided by A. McKenzie (MRC Laboratory of Molecular Biology, Cambridge, United Kingdom) and maintained on a 129Ola/C57BL/6 (F2) background (17). The IL-13Rα2–deficient mice were generated as described (38) and backcrossed onto the C57BL/6 and BALB/c backgrounds. The IL-13Rα2–deficient mice were either provided by Wyeth-Genetics Institute or shipped directly from The Jackson Laboratory. Stat6-deficient mice were generated as previously described (40) and provided by W.E. Paul (NIH, Bethesda, MD). Age- and sex-matched mice were housed in an NIH American Association for the Accreditation of Laboratory Animal Care–approved animal facility. All mice were infected percutaneously through the tail with 25–30 cercariae of a Puerto Rican strain of *S. mansoni* (NMRI) obtained from infected *Biomphalaria glabrata* snails (Biomedical Research Institute). In some experiments, mice were sensitized with *S. mansoni* eggs extracted from the livers of infected mice. Sensitization of mice with eggs and rIL-12 was previously described in detail (41). In brief, groups of 10 mice were injected intraperitoneally with 5,000 eggs on three occasions separated by 2-wk intervals. Animals were also injected intraperitoneally with either saline or rIL-12 (0.25 μg/dose) consecutively for 5 d beginning on the day of each immunization and then infected 2–4 wk after the last IL-12 injection. For the induction of pulmonary granulomas, mice were challenged with 5,000 eggs intravenously. Mice were killed in groups of five on days 7 and 11 after challenge. Some groups were also treated with 0.25 μg rIL-12 on days 0, 1, 3, 4, and 6. rIL-12 and rIL-13 were

*Abbreviations used in this paper: CCCA, Cincinnati cytokine capture assay; HPRT, hypoxanthine-guanine phosphoribosyl transferase; SEA, soluble egg antigen; sIL-13Rα2-Fc, soluble IL-13Rα2-Fc.

provided by Wyeth-Genetics Institute. Soluble egg antigen (SEA) was purified from homogenized *S. mansoni* eggs, as previously described (10). The sIL-13Rα2-Fc fusion protein and control-Fc were prepared as previously described (29) and provided by Wyeth-Genetics Institute. In the IL-13 blocking studies, animals were treated between 6 and 12 wk after infection by intraperitoneal injection of 0.5 ml PBS containing 200 μg/mouse sIL-13Rα2-Fc every other day, the optimal dose as determined in previous studies (42). Animals were perfused at the time of death to determine worm and tissue egg burdens as previously described (10).

Histopathology and Fibrosis Measurement. The size of hepatic granulomas was determined in histologic sections stained by Wright's Giemsa stain (Histopath of America). ~30 granulomas per mouse were included in all analyses. The percentages of eosinophils, mast cells, and other cell types were evaluated in the same sections. The frequency of mast cells was evaluated on a scale from 0–4, with 0 being low and 4 being a high frequency. The number of schistosome eggs in the liver and gut and the collagen content of the liver, determined as hydroxyproline, were measured as previously described (10). Specifically, hepatic collagen was measured as hydroxyproline by the technique of Bergman and Loxley (43) after hydrolysis of a 200-mg portion of liver in 5 ml of 6 N HCl at 110°C for 18 h. The increase in hepatic hydroxyproline was positively related to egg numbers in all experiments and hepatic collagen is reported as the increase above normal liver collagen in micromoles per 10,000 eggs: (infected liver collagen − normal liver collagen)/liver eggs $\times 10^{-4}$ or micromoles per worm pair. Fibrosis was also evaluated histologically using liver sections stained with picrosirius red. The same individual scored all histologic features and had no knowledge of the experimental design.

Isolation and Purification of RNA and RT-PCR. Liver tissues were homogenized in TRIzol reagent (Invitrogen) using a tissue polytron (Omni International Inc.) and total RNA was extracted according to the recommendations of the manufacturer. An RT-PCR procedure was used to determine relative quantities of mRNA for several cytokine and cytokine receptor genes after reverse transcription of 1 μg RNA as previously described (44). The primers and probes for all genes were published previously (44), except IL-13Rα1: 5′-GCA-GCC-TGG-AGA-AAA-GTC-GTC-AAT-3′ (sense), 5′-ACA-GCG-TCG-GCA-AGA-ACA-CCA-3′ (antisense); IL-13Rα2: 5′-ATG-GCT-TTT-GTG-CAT-ATC-AGA-TGC-T-3′ (sense), 5′-CAG-GTG-TGC-TCC-ATT-TCA-TTC-TAA-T-3′ (antisense); γc chain: 5′-ATG-TCC-AGT-GCG-AAT-GAA-GA-3′ (sense), 5′-CTC-CGA-ACC-CGA-AAT-GTG-TA-3′ (antisense); and IL-4Rα1: 5′-GAG-TGA-GTG-GAG-TCC-TAG-CAT-C-3′ (sense), 5′-GCT-GAA-GTA-ACA-GAA-CAG-GC-3′ (antisense). The PCR cycles used for each cytokine were as follows: IL-13 (33), IL-4 (34), IL-5 (31), IFN-γ (29), IL-13Rα1 (28), IL-13Rα2 (30), IL-4Rα1 (27), γc chain (27), and hypoxanthine-guanine phosphoribosyl transferase (HPRT; reference 23). The amplified DNA was analyzed by electrophoresis, Southern blotting, and hybridization with nonradioactive cytokine-specific probes as previously described (44). The PCR products were detected using an enhanced chemiluminescence detection system (Amersham Biosciences). The chemiluminescent signals were quantified using a flat bed scanner (model 600 ZS; Microtek). Arbitrary densitometric units were calculated by dividing the cytokine or cell surface marker OD units by the individual HPRT OD units and multiplying by 100. In some experiments, real-time PCR was conducted on an ABI Prism 7900 sequence detection system (Applied Biosystems) using SYBR Green PCR Master Mix after RT of 1 μg RNA. The amount of PCR product was determined by the Comparative Ct Method as described by the manufacturer, in which each sample was normalized to HPRT and expressed as a fold increase or decrease versus unchallenged controls.

Western Blot Analysis of IL-13Rα2. Sera was diluted with 1 vol cell lysis buffer (Tris-buffered saline [20 mM Tris, 150 mM NaCl, pH 7.5], 1% Triton X-100, 40 mg of iodoacentamide per 25 ml, 1 tablet protease inhibitor cocktail; Boehringer). Three to five million BaF3/IL-13Rα2 cells were lysed in 1.5 ml lysis buffer. IL-13Rα2 was precipitated with 2.5 μg biotinylated Chinese hamster ovary murine IL-13 and streptavidin agarose beads (streptavidin coupled to agarose; Pierce Chemical Co.). The agarose beads were washed three times with lysis buffer with NaCl adjusted to 400 mM followed by two washes with PBS. Samples were reduced and separated on a 12% SDS-PAGE and then transferred to polyvinylidene difluoride (NEN Life Science Products) by semi-dry electroblotting. The blot was blocked with Tris-buffered saline 1% Tween-20/4% BSA and then incubated with polyclonal rabbit sera to murine IL-13Rα2 (5 μg/ml; Wyeth-Genetics Institute). Peroxidase-labeled goat anti–rabbit IgG (1:20,000; Jackson ImmunoResearch Laboratories) was added as a second step. The blot was developed with enhanced chemiluminescence reagents (Amersham Biosciences) and exposed on Hyperfilm (Amersham Biosciences).

In Situ Hybridization. Sections of paraffin-embedded tissue were deparaffinized with xylene, two changes, 3 min each, and rehydrated to water. After a rinse in RNase-free water and PBS, permeabilization was performed by incubation with 0.2% Triton X-100/PBS for 15 min. After two washes with PBS, the sections were immersed in 0.1 M Tris and 50mM EDTA, pH 8.0 (Sigma-Aldrich), prewarmed at 37°C containing 5 μg/ml proteinase K for 15 min. Proteinase K activities were stopped by 0.1 M glycine/PBS for 5 min followed by a postfixation with 4% paraformaldehyde for 3 min and then a PBS rinse. To prevent nonspecific electrostatic binding of the probe, sections were immersed in 0.25% acetic anhydride and 0.1 M triethanolamine solution, pH 8.0, for 10 min followed by 15 s in 20% acetic acid at 4°C. After three changes in PBS of 5 min each, sections were dehydrated through 70, 90, and 100% ethanol, each at 3 min. The sections were completely air-dried before 40 μl prehybridization buffer was applied, covered with parafilm, and incubated at 52°C for 30 min to reduce nonspecific binding. Parafilm was removed and 40 μl hybridization buffer containing 5 ng/μl digoxigenin-labeled probe was applied to each section, recovered with parafilm, and incubated overnight at 52°C in a humid chamber. To generate the riboprobes, a 23-nucleotide T7 promoter was added to the 5′ or 3′ end to generate the template for making either the antisense or sense riboprobe. The T7 sequence used was taatacgactcactatagggaga. IL-13Rα1 (sequence data are available from GenBank/EMBL/DDBJ under accession no. S8096) 5′ probe: ggagtcctcctgaaggagccag, 3′ probe: ggtcaacacattgcttgttcc, used to generate a 403-bp riboprobe; IL-13Rα2 (sequence data are available from GenBank/EMBL/DDBJ under accession no. NM_008356) 5′ probe: gatcatgccttacagtgtgc, 3′ probe: ggagcgaatggagtgaagagg, used to generate a 450-bp riboprobe; and IL-4Rα (sequence data are available from GenBank/EMBL/DDBJ under accession no. M29854) 5′ probe: ggcggtccaatcagacagatacc, 3′ probe: ctcctgcctctgcatcccgttg, used to generate a 463-bp riboprobe.

Parafilm was carefully removed and the sections were placed in a Biogenex Genomx 6000 automatic staining system. Sections were washed in 2× SSC/0.1% SDS (both from Sigma-Aldrich) at

room temperature, four changes at 5 min each. To ensure only specific hybridization signal remains, sections were washed in a high stringency solution containing 0.1× SSC/0.1% SDS at 52°C, two changes at 5 min each. To reduce endogenous peroxidase staining, the sections were incubated in 3% H_2O_2 for 15 min followed by three washes in buffer. The probe was detected with antidigoxigenin antibody conjugated to horseradish peroxidase complex (Roche) diluted 1:500 in 2% normal sheep serum/0.1% Triton X-100 for 1 h. The biotinylated complex was amplified using the Tyramide Amplification System (Biogenex). Sections were incubated with trichostatin A for 5 min followed by five washes in buffer. The trichostatin A complex was then amplified further by an incubation with horseradish peroxidase for 15 min followed by five washes in buffer. The amplified product was developed with 3,3′-diaminobenzidine (Vector Laboratories) for 10 min, washed in water, stained briefly with Mayers' hematoxylin (Sigma-Aldrich), dehydrated through graded alcohol into xylene, and mounted in DPX mountant before microscopic examination.

ELISPOT and Cincinnati Cytokine Capture Assay (CCCA). Single cell suspensions of splenocytes were plated in 24-well plates (4×10^6 cells/ml) and stimulated with 20 μg/ml SEA. After 24 h, cells were harvested and plated (10^5, 5×10^4, and 10^4 cells/well) in 96-well plates previously coated with different cytokine-specific Abs at a final concentration of 10 μg/ml (anti–IFN-γ, anti–IL-4, anti–IL-5, or anti–IL-13) and subsequently blocked with 5% FCS. Cells were incubated overnight at 37°C in an atmosphere of 5% CO_2. After washing with PBS/Tween 20, plates were incubated with biotinylated anticytokine Ab (1:1,000 dilution) for 2 h at 37°C. Plates were washed and incubated with alkaline phosphatase avidin (1:5,000 dilution) for 1 h at room temperature. Plates were developed using 5-bromo-4-chloro-3-indolylphosphate-agarose and spots were counted the next day using an inverted microscope. The CCCA assay was performed as previously described (45). In brief, 10 μg biotinylated anti–IFN-γ or anti–IL-4 mAbs were injected intravenously into 9-wk–infected mice. Mice were bled 18 h later and serum was collected for the detection of IFN-γ and IL-4 by ELISA.

Serum Ab Isotype Analysis. Isotype-specific Ab titers were evaluated by indirect ELISA. Immulon 4 plates were coated with 10 μg/ml SEA (50 μl/well) diluted in PBS and serum samples were analyzed using serial twofold dilutions. Second step horseradish peroxidase–conjugated rabbit anti–mouse IgM, IgG, IgG1, IgG2a, and IgG2b Abs (Zymed Laboratories) were used at a 1:1,000 dilution. The absorbance was read at 405 nm using a Vmax Kinetic Microplate Reader (Molecular Devices) after adding 100 μl ABTS/H2O2 one step substrate.

Statistics. Hepatic fibrosis (adjusted for egg number) decreases with increasing intensity of infection (worm pairs). Therefore, these variables were compared by analysis of covariance, using the log of total liver eggs as the covariate and the log of hydroxyproline per egg. Variables that did not change with infection intensity were compared by one way ANOVA or by Student's *t* test. Changes in cytokine mRNA expression, ELISPOT assays, and granuloma size were evaluated by ANOVA. Results were considered significant where $P < 0.05$.

Results

Transition from Acute to Chronic S. mansoni Infection Is Characterized by Increased Fibrosis and IL-13Rα2 Expression and Decreased IL-4Rα mRNA in the Liver. The progression of fibrotic liver pathology after infection with *S. mansoni* cercariae was evaluated in several strains of mice after infection (46). In addition, liver RNA was isolated so that IL-4/IL-13 receptor mRNA expression could be examined and correlated with pathology. Eggs were deposited by adult paired parasites starting on week 4 or 5 of infection and a subset trapped in the liver, where they trigger a vigorous inflammatory response, peaking approximately 8 or 9 wk after infection. The egg-induced granulomatous response is also accompanied by a marked deposition of collagen, which continues to increase in a linear fashion into the chronic phase of infection. In these experiments, fibrosis was evaluated at multiple time points after infection by measuring hydroxyproline levels in the liver. As shown in Fig. 1, all three strains developed significant fibrosis by week 9 and this continued to increase through 16 wk after infection.

S. mansoni–infected C57BL/6, C3H/HeN, and BALB/c mice all display increases in IL-4 and IL-13 expression that correlate with the development of fibrotic pathology in the liver (7). However, changes in IL-4 and IL-13 receptor expression could also affect the activity of these cytokines. Therefore, in the following experiments, we investigated whether IL-4Rα, γc, IL-13Rα1, and IL-13Rα2 mRNA expression was regulated in the liver after infection with *S. mansoni*. Liver RNA was isolated at multiple time points after infection and RT-PCR analysis was performed. The IL-13Rα1 chain, which binds IL-4 and IL-13 with equal affinity (26), was expressed constitutively in the liver of all uninfected mice (unpublished data). Although there was some indication that levels were decreasing slightly, particularly at the acute stage after infection in BALB/c and C3H/HeN mice, in general, expression remained relatively constant through week 16 (Fig. 2 D). The common γ chain exhibited a similar profile in all three strains, showing little or no change in expression after infection (Fig. 2 C). In marked contrast, however, results for the IL-4Rα and IL-13Rα2 chains were striking. The IL-13Rα2 chain was expressed at very low levels in the liver at early stages of infection. However, by the acute stage after infection, a marked increase in IL-13Rα2 mRNA expression was observed in all three strains, which peaked on week 12 and declined slightly by week 16 (Fig. 2 B). In contrast to the IL-13Rα2 chain, the IL-4Rα chain exhibited an opposite pattern of expression after infection (Fig. 2 A). A high level of IL-4Rα1 mRNA expression was observed in the liver before the onset of egg laying, but was down-regulated on week 9 and remained at relatively low levels throughout the 16 wk of study. The pattern was similar in all three

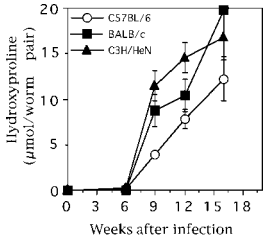

Figure 1. Kinetics of hepatic fibrosis after infection with *S. mansoni*. Groups of C57BL/6, BALB/c, and C3H/HeN mice were infected with 25–30 *S. mansoni* cercariae. 5–10 animals per group were killed at the time points specified. Fibrosis was assessed by the amount of hydroxyproline in micromoles detected in the liver per worm pair. Each data point shows the average values per group ± SE.

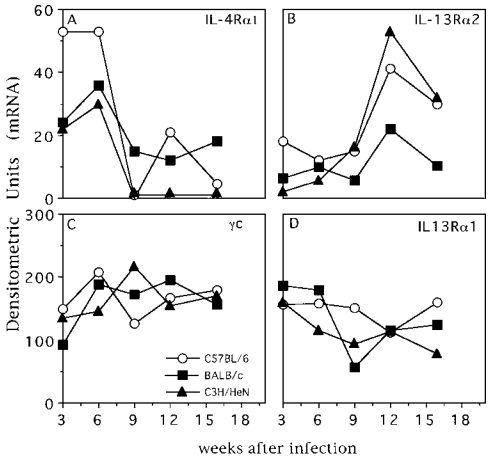

Figure 2. Kinetics of IL-4/IL-13 receptor mRNA expression in the liver after infection with *S. mansoni*. Groups of C57BL/6, BALB/c, and C3H/HeN mice were infected with 25–30 *S. mansoni* cercariae. 5–10 animals per group were killed at the time points specified. RNA was extracted from the liver of individual mice at different time points and RT-PCR was performed as described in Materials and Methods for IL-4Rα1 (A), IL-13Rα2 (B), γc chain (C), and IL-13Rα1 (D). Average densitometric units from 5 to 10 mice per time point are shown.

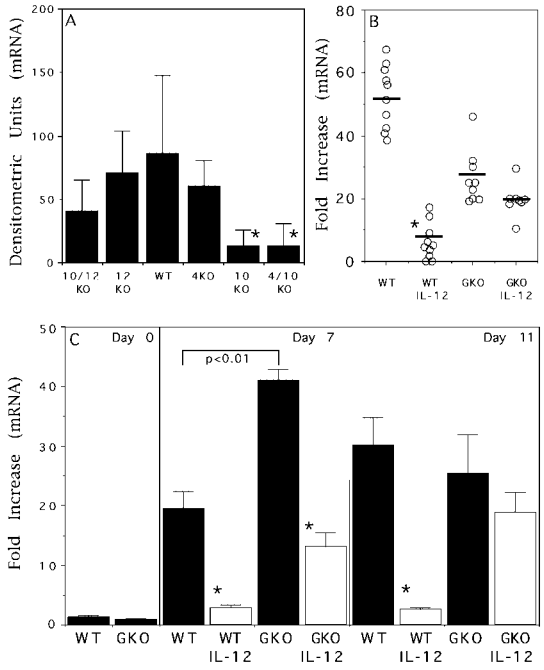

Figure 3. IL-13Rα2 mRNA expression is regulated by the type 1/type 2 cytokine response. (A) All mice (IL-10/IL-12–deficient mice [10/12KO], IL-12–deficient mice [12KO], WT, IL-4–deficient mice [4KO], IL-10–deficient mice [10KO], and IL-4/IL-10–deficient mice [4/10KO]) were infected with 25–30 *S. mansoni* cercariae. 10 animals per group were killed 9 wk after infection. RNA was extracted from the liver and RT-PCR was performed for IL-13Rα2. Bars, average densitometric units ± SD; *, significant difference when compared with WT values as determined by Student's *t* test. $P < 0.05$. (B) C57BL/6 (WT) and IFN-γ–deficient (GKO) mice were sensitized with eggs and IL-12 (egg/IL-12) or not and infected with cercariae as described in Materials and Methods. On week 9, mice were killed and IL-13Rα2 mRNA levels were determined in the liver by real-time PCR. *, significant difference when compared with the respective non–IL-12–treated control group as determined by Student's *t* test. $P < 0.05$. (C) Naive C57BL/6 (WT) and IFN-γ–deficient (GKO) mice were injected intravenously with 5,000 schistosome eggs and treated with saline (filled bars) or IL-12 (open bars) as described in Materials and Methods. Mice were killed on days 0, 7, and 11 after challenge and total lung RNA was isolated for the detection of IL-13Rα2 mRNA by real-time PCR. *, significant difference when compared with the respective non–IL-12–treated control group as determined by Student's *t* test. $P < 0.05$.

strains. When viewed together, these data demonstrate that the increasing level of hepatic fibrosis observed in chronic infection (Fig. 1) correlates most closely with an increase in IL-13Rα2 expression.

IL-13Rα2 Production Is Controlled by the Type 1/Type 2 Cytokine Expression Profile. Because expression of IL-13Rα2 correlated with the development of fibrosis, we were interested in understanding the mechanisms that control its expression. In particular, we examined whether type 1 or type 2 cytokines influence expression of the receptor. In previous studies, we showed that IL-10/IL-4– and IL-10/IL-12–deficient mice develop exaggerated and highly polarized type 1 and type 2 cytokine responses, respectively, after infection with *S. mansoni* (39). As such, these mice provided ideal tools to examine the role of cytokines in the regulation of the IL-13Rα2 chain during an ongoing inflammatory response. In these experiments, single and double cytokine-deficient mice were infected and expression of IL-13Rα2 mRNA was examined in the liver. Of interest, the only mice that failed to show a significant up-regulation of receptor expression after infection were the IL-10 and IL-10/IL-4 double deficient mice (Fig. 3 A). These mice, in contrast to the other animals, showed either a mixed Th1/Th2 or highly polarized Th1-type response after infection, respectively (6), suggesting that a response skewed toward Th2 cytokines is required for IL-13Rα2 expression.

To further test this hypothesis, we sensitized WT C57BL/6 mice with eggs and IL-12 before infection to deviate the normal egg-induced Th2 response to a more Th1-dominant reaction (9, 47). In addition, to evaluate the contribution of IFN-γ specifically, we conducted similar immune deviation experiments in IFN-γ–deficient mice. Consistent with results generated in IL-10 and IL-10/IL-4–deficient mice, the egg/IL-12–sensitized WT mice showed more than a sixfold reduction in IL-13Rα2 mRNA expression when compared with nonsensitized WT controls (Fig. 3 B). Although non–IL-12–treated IFN-γ–deficient mice also displayed a partial reduction (less than twofold), the suppressive effect mediated by IL-12 was almost completely ablated in the KO animals. Cytokine assays confirmed that type 2 cytokine expression, including IL-4, IL-5, and IL-13, was reduced whereas IFN-γ mRNA expression increased in the livers of the egg/IL-12–sensitized WT mice (unpublished data). To further dissect the individual roles of IFN-γ and IL-12, additional studies were also conducted in the primary lung granuloma model (47), where the initial induction of IL-13Rα2 expression could be examined. In these studies, purified eggs were injected intravenously into WT and IFN-γ–deficient mice and IL-13Rα2 mRNA expression was monitored in the lung by

real-time PCR at 0, 7, and 11 d after challenge. Some groups were also treated with rIL-12 during the first week. On day 11 (Fig. 3 C), the results closely mirrored the pattern observed in the liver of infected mice (Fig. 3 B), with WT and IFN-γ–deficient mice showing significantly upregulated IL-13Rα2 expression and only WT mice showing reduced expression after rIL-12 treatment. Strikingly however, on day 7, 1 d after the last treatment with rIL-12, the non–IL-12–treated IFN-γ–deficient mice displayed an enhanced IL-13Rα2 response whereas WT and IFN-γ–deficient mice both showed reduced IL-13Rα2 mRNA levels after treatment with IL-12. These later findings indicate that IL-12 exhibits some suppressive activity that is IFN-γ independent. Nevertheless, this activity appears to be transient because no suppression was observed in the IFN-γ–deficient mice on day 11, 5 d after the last treatment with IL-12.

Finally, in another series of experiments, we examined whether the ligand for IL-13Rα2 was itself a stimulus for receptor expression. In one experiment, WT and IL-13–deficient mice were infected with *S. mansoni* and IL-13Rα2 mRNA expression was evaluated in the liver tissues. As shown in Fig. 4 A, IL-13Rα2 expression decreased by ~80% in the absence of IL-13. Finally, a more direct approach was used to determine whether recombinant IL-13 alone could induce IL-13Rα2 expression in the liver. In these experiments, naive WT mice were injected with a single dose of rIL-13 administered intraperitoneally and receptor expression was monitored in the liver at several time points. As shown in Fig. 4 B, receptor expression was upregulated as early as 3 h after injection. In the example shown, peak expression occurred at 6 h and declined thereafter. Additional studies, however, showed that IL-13Rα2 expression remained above basal levels for as long as 72 h after exposure to rIL-13 (unpublished data).

IL-13Rα2 can also be released from the surface of cells and exist as a soluble form in the serum (48). To determine whether the soluble form of the receptor was produced after infection, Western blots were performed on sera obtained from infected and uninfected WT and IL-13/IL-4– and Stat6-deficient mice. As shown in Fig. 4 C, lane 1 shows control staining for both the membrane and soluble forms of the receptor (arrows). Unlabeled murine IL-13 was also used as a competitor during the immunoprecipitation step to demonstrate the specificity of the reaction (Fig. 4 C, lane 2). Interestingly, a low but detectable level of soluble receptor was found in the serum of all uninfected mice (Fig. 4 C, lanes 4, 6, and 8). However, only WT mice showed a markedly increased level of the soluble form after infection (Fig. 4 C, lane 3), further suggesting that IL-13Rα2 expression is highly dependent upon IL-4/IL-13– and Stat6-dependent signaling pathways.

In situ hybridization was also performed on liver sections prepared from 9-wk–infected mice so that the pattern of expression of IL-13Rα2, IL-13Rα1, and IL-4Rα might be determined. As shown in the photomicrographs (Fig. 5), all three receptors showed a unique pattern of expression in the liver. Staining for IL-4Rα was primarily restricted to

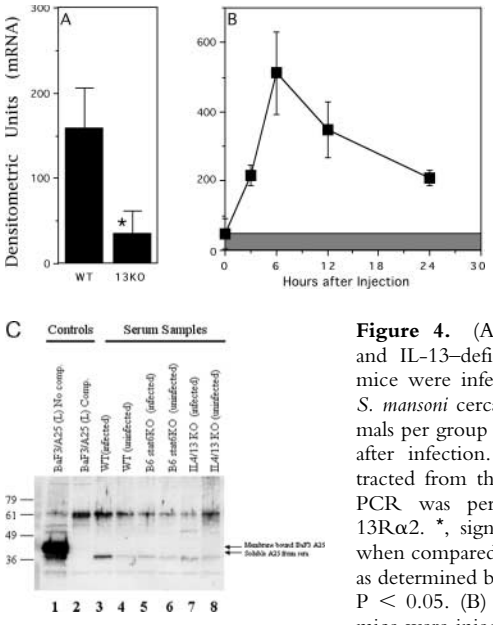

Figure 4. (A) WT (WT F2) and IL-13–deficient (IL-13KO) mice were infected with 25–30 *S. mansoni* cercariae and 10 animals per group were killed 9 wk after infection. RNA was extracted from the liver and RT-PCR was performed for IL-13Rα2. *, significant difference when compared with WT values as determined by Student's *t* test. $P < 0.05$. (B) Naive C57BL/6 mice were injected with a single 10-μg dose of rIL-13 and liver RNA was prepared at the various time points indicated to determine the level of IL-13Rα2 mRNA expression. The shaded bar denotes the background levels observed in unexposed mice. Average densitometric unit per group ± SD is shown at each time point ($n = 5$ mice/time point). (C) Immunoprecipitation/Western of sera from schistosome-infected and -uninfected mice. Mice (IL-4/IL-13–deficient mice [IL4/13 KO], Stat6-deficient [B6 Stat6KO], and WT) were infected with 25–30 *S. mansoni* cercariae and serum was collected 9 wk after infection. All sera were precipitated with biotinylated murine IL-13 and streptavidin agarose beads overnight. The sample was treated with PNGase F, resolved on 12% reducing gel, blotted to polyvinylidene difluoride, and then IL-13Rα2 detected with rabbit anti–mouse A25 and goat anti–rabbit horseradish peroxidase. Comp, competition during the immunoprecipitation step with unlabeled murine IL-13 (note, no IL-13Rα2 [A25] band); arrows, soluble and membrane A25 (IL-13Rα2) have two different mobilities.

the granulomas where lymphocytes are concentrated (Fig. 5 A) whereas staining for IL-13Rα2 was observed more densely at the periphery of the lesions where fibroblast proliferation and activation occurs (C). Positive staining for IL-13Rα1, in contrast to the other receptors, was much more ubiquitous in the liver and not necessarily restricted to the granulomatous lesions (Fig. 5 E). Control probes for each receptor confirmed the specificity of the staining (Fig. 5, B, D, and F).

Evidence of Decoy Activity: IL-13Rα2–deficient Mice Develop Severe Liver Fibrosis after Infection with S. mansoni. IL-13Rα2–deficient mice were generated as previously described (38) so that the functional role of the endogenous IL-13Rα2 could be elucidated in vivo. Animals backcrossed to the C57BL/6 and BALB/c backgrounds were infected percutaneously with 25 *S. mansoni* cercariae and examined for several immunologic and parasitologic changes at the time of death. Because some studies suggested that the immune status of the mouse may affect the development and/or fecundity of worms (49, 50), we first determined whether worm or egg burdens were affected by the IL-13Rα2 deficiency (Table I). Mice from both

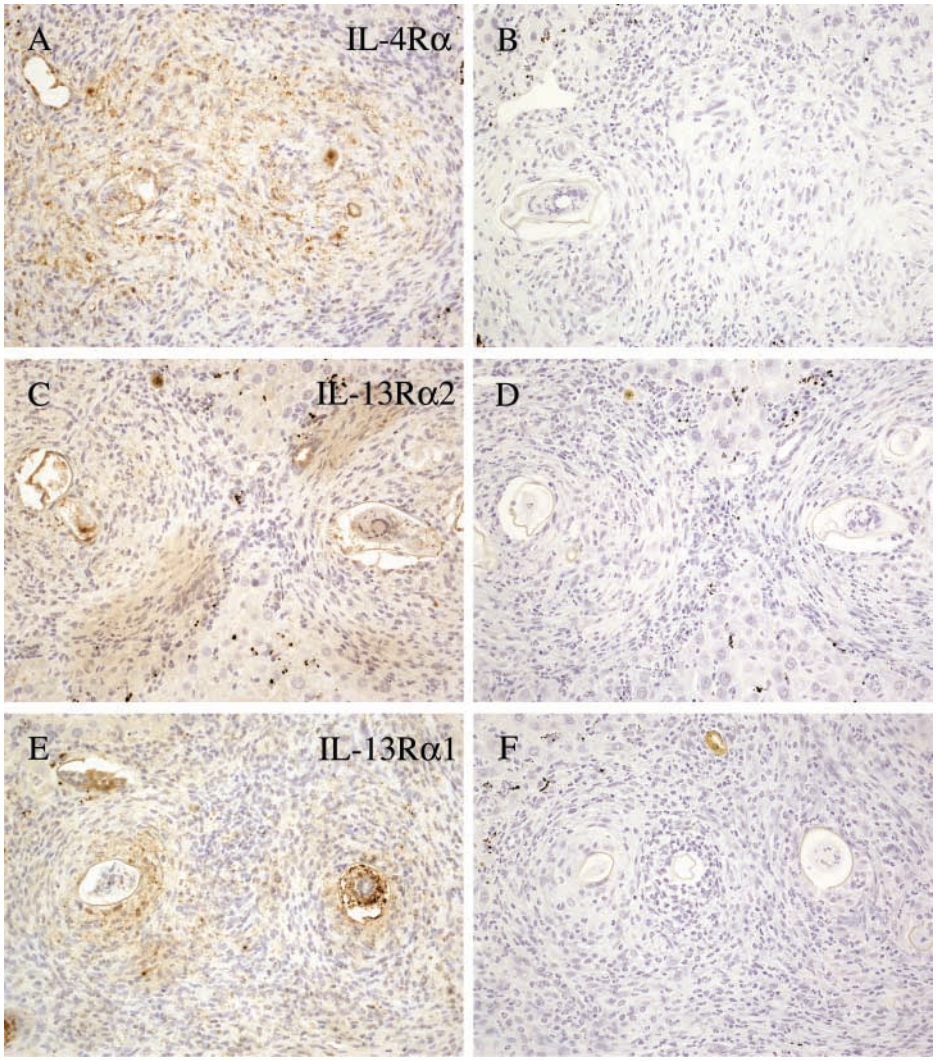

Figure 5. Localization of IL-4/IL-13 receptor expression in the livers of infected mice. Liver sections from 9-wk–infected BALB/c mice were fixed in paraformaldehyde and in situ hybridization was performed for IL-4Rα, IL-13Rα2, and IL-13Rα1 mRNA. Antisense (A, C, and E) and sense strand (B, D, and F) riboprobes were used in the hybridization reaction using serial tissue sections. The brown areas denote positive staining for each receptor. Each section contains at least one granuloma with a miracidium-containing egg at the center. ×20.

backgrounds were perfused at the time of death, and worm pairs and total worm burden were determined revealing no differences in either parameter. We also noted no difference in the tissue egg burden (Table I). Liver sections from infected WT and IL-13Rα2–deficient mice were also examined microscopically for granuloma size and recruitment of eosinophils and mast cells to the lesions (Fig. 6). Although the C57BL/6 and BALB/c strains showed differences in the number of recruited eosinophils (Fig. 6 B) and mast cells (C), there were no significant differences observed between the WT and IL-13Rα2–deficient mice on either background. This was also true for macrophages and lymphocytes, which made up 35.3 and 7.55% of granuloma cells in WT C57BL/6 mice and 40.8 and 8.2% in IL-13Rα2–deficient mice, respectively. Similar findings were observed with BALB/c WT and IL-13Rα2–deficient mice (unpublished data). Extensive flow cytometric analyses of isolated granuloma cells also revealed no major differences between the KO and WT mice (unpublished data). The average size of granulomas was also completely unaffected by the IL-13Rα2 deficiency (Fig. 6 A).

The extent of hepatic fibrosis after infection was also assessed by measuring hydroxyproline levels in the liver (Fig. 7) and staining tissue sections with the collagen-specific

Table I. *Parasitological Measurements in WT and IL-13-Rα2–deficient Mice at Week 9 after Infection*

	Total worms	Worm pairs	Eggs/worm pair (×1,000)
	N (SEM)	N (SEM)	N (SEM)
BALB/c WT	12.8 (1.05)	5.25 (0.5)	9.81 (1.49)
IL-13Rα2 KO	11.4 (1.46)	4.30 (0.86)	9.42 (0.77)
C57BL/6 WT	19.1 (2.32)	9.40 (1.1)	5.78 (0.42)
IL-13Rα2 KO	16.0 (1.92)	6.50 (1.2)	6.32 (0.78)

All data are means for each group ± SEM.
N, number.

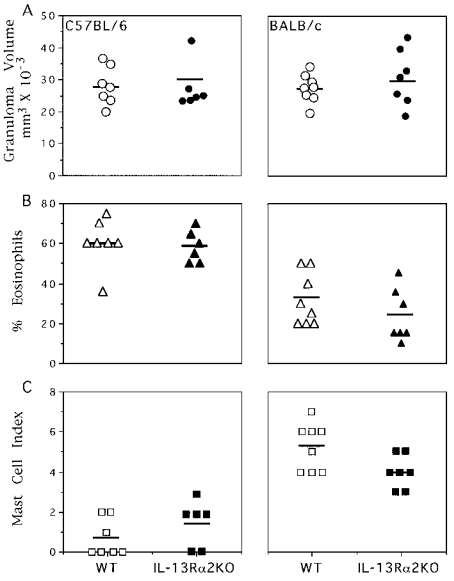

Figure 6. IL-13Rα2 deficiency does not affect the size or cellular composition of granulomas. C57BL/6 and BALB/c WT and IL-13Rα2–deficient mice were infected with 25–30 cercariae. Granuloma size (A), tissue eosinophilia (B), and mast cell index (C) were assessed 9 wk after infection. Six to eight mice were included in each group and the values for individual animals are shown. Bars denote the means. No significant differences were noted.

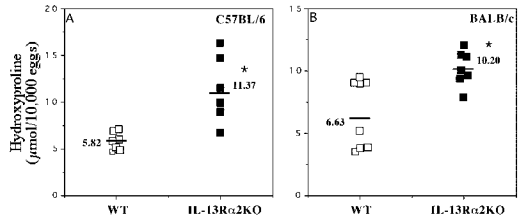

Figure 7. Hepatic fibrosis increases in the absence IL-13Rα2. (A) C57BL/6 and (B) BALB/c WT and IL-13Rα2–deficient mice were infected with 25–30 cercariae and hepatic fibrosis was assessed by hydroxyproline assay 9 wk after infection. Six to eight mice were included in each group and the values for individual animals are shown. Bars, the means; *, significant difference when compared with WT values as determined by ANOVA. $P < 0.05$.

stain picrosirius red (unpublished data). Strikingly, both approaches showed that IL-13Rα2–deficient mice on either background were much more susceptible to the development of fibrosis compared to the respective WT strains. Even more interesting was the pattern of fibrosis in the IL-13Rα2–deficient mice. In WT animals, picrosirius red staining was largely restricted to the areas surrounding the granulomas. The IL-13Rα2–deficient mice, on the other hand, showed a pattern of fibrosis that extended well beyond the boundaries of the granuloma. Indeed, intense staining was easily observed in infected IL-13Rα2–deficient mice in areas of the liver where no egg-induced lesion formation was obvious. No such staining was seen in the parenchymal tissues of infected WT animals at this time point.

To compliment the hydroxyproline data and to further investigate the mechanisms involved, we examined the mRNA expression profiles of several genes that are thought to be directly involved in the fibrotic process. These included procollagen I, matrix metalloproteinase 12, tissue inhibitor of matrix metalloproteinase 1, TGF-β1, as well as arginase 1 (51–53), which is induced by IL-4/IL-13 and regulates proline production in macrophages (53, 54). Consistent with the increase in liver hydroxyproline, the IL-13Rα2–deficient mice displayed a threefold increase in procollagen I mRNA expression when compared with WT mice 12 wk after infection. Tissue inhibitor of matrix metalloproteinase 1 mRNA expression was also significantly elevated whereas expression of matrix metalloproteinase 12 mRNA decreased nearly threefold relative to WT mice. TGF-β1 mRNA expression was similar in both groups (unpublished data). Finally, preliminary studies examining arginase 1 revealed a two- to fourfold increase in pulmonary arginase 1 mRNA levels in the KO versus WT mice after an intravenous challenge with schistosome eggs, further confirming the conclusion that the profibrotic activity of IL-13 is increasing in the absence of the IL-13Rα2.

Severe Fibrotic Response in IL-13Rα2–deficient Mice Is Not Associated with Increased Type 2 Cytokine Production. Numerous studies have shown that development of fibrosis in murine schistosomiasis is highly type 2 cytokine dependent (6, 9, 55) and recent studies have identified IL-13 as the key fibrogenic mediator (7, 11, 12). As such, increased IL-4/IL-13 production could be one mechanism by which fibrogenesis is altered in the absence of IL-13Rα2 because signaling through the type I and type II IL-4/IL-13 receptors would remain intact in these animals. Therefore, we examined the type 1/type 2 cytokine profile both locally and systemically in WT and IL-13Rα2–deficient mice after infection. ELISPOT assays performed on splenocytes, however, showed no significant change in the frequency of SEA-specific IFN-γ–, IL-4–, IL-5–, or IL-13–producing cells (unpublished data). IFN-γ and IL-4 levels were also examined in the serum of infected mice using the CCCA and Luminex assays (45, 56), however, no significant differences were detected between the WT and IL-13Rα2–deficient mice. IL-4 was just at the threshold of detection in most animals whereas a low but significant IFN-γ response (WT average, 52.6 pg/ml and IL-13Rα2 KO average, 29.6 pg/ml) was observed in both groups. The local cytokine response was also examined in the granulomatous tissues by RT-PCR. Here, IFN-γ mRNA expression was again unaffected by the absence of IL-13Rα2 whereas, unexpectedly, expression of both IL-4 and IL-13 decreased significantly (Fig. 8 A). We also examined whether expression of the IL-4/IL-13 receptor chains was altered in the IL-13Rα2–deficient mice. As expected, IL-13Rα2 mRNA expression significantly increased in WT mice after infection whereas no IL-13Rα2 mRNA was detectable in the KO mice (Fig. 8 B). Consistent with earlier findings, high levels of IL-13Rα1 and γc were observed in both un-

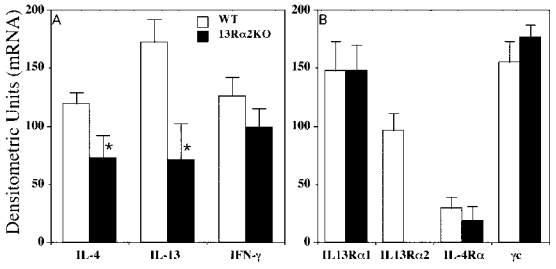

Figure 8. IL-4 and IL-13 mRNA expression decreases in IL-13Rα2–deficient mice. (A) WT C57BL/6 (open bars) and IL-13Rα2–deficient (filled bars) mice were infected with 25–30 cercariae. RT-PCR was performed for IL-4, IL-13, and IFN-γ on liver tissues as described in Materials and Methods. *, significant difference when compared with WT values as determined by Student's *t* test. $P < 0.05$. (B) RT-PCR for IL-13Rα1, IL-13Rα2, IL-4Rα, and γc chains was performed on the same tissues. Six to eight mice were killed per group and the average arbitrary densitometric units are shown ± SD. No significant differences were found between the WT and IL-13Rα2–deficient mice. Similar results were obtained with tissues from mice on the BALB/c background.

infected (not depicted) and infected mice (Fig. 8 B), and there was no evidence that either gene was affected by the absence of IL-13Rα2. The same finding was true for IL-4Rα mRNA, although expression of this receptor gene was found at elevated but lower levels than the other receptor chains at this postinfection time point.

The egg-specific antibody response was also examined in the serum of infected WT and IL-13Rα2–deficient mice. Both groups showed similar titers of total anti–SEA-specific Ig (Fig. 9). IgM titers were also similar in both animals whereas IgG2a and IgG2b titers decreased slightly but not significantly in IL-13Rα2–deficient versus WT mice. We did, however, note a consistent and highly significant decrease in the IgG1 antibody titer in receptor-deficient animals (Fig. 9) whereas levels of SEA-specific IgE were unchanged (not depicted).

Decoy Function Is Restored and Fibrosis Decreased in IL-13Rα2–deficient Mice after Administration of sIL-13Rα2-Fc Protein. In a final series of experiments, a soluble IL-13 antagonist composed of the IL-13Rα2 chain (29) was administered to IL-13Rα2–deficient mice to determine whether the increase in hepatic fibrosis observed in receptor-deficient animals could be reversed by restoring IL-13Rα2 activity. In these experiments, IL-13Rα2–deficient mice were infected for 12 wk and treated with sIL-13Rα2-Fc or control-Fc protein for 6 wk after the onset of egg laying (weeks 6–12). Thus, in contrast to previous experiments, these studies examined the function of the decoy receptor at a more chronic time point after infection. Because the RT-PCR results presented above (Fig. 8 A) show decreasing levels of IL-13 mRNA in IL-13Rα2–deficient versus WT mice, we initially examined whether the decoy receptor was influencing IL-13 expression in serum. Interestingly, quite high levels of IL-13 were detectable in infected WT mice (Fig. 10 B) whereas <50 pg/ml IL-13 was observed in uninfected mouse serum (not depicted). Consistent with results in the liver, the levels of IL-13 protein were much lower in IL-13Rα2–deficient animals. Strikingly, however, serum levels of IL-13 increased dramatically when the KO mice were treated with the sIL-13Rα2-Fc protein. Consistent with findings from acute time points (Fig. 7), mice deficient in IL-13Rα2 again developed significantly more fibrosis than infected WT animals (Fig. 10 A). Of more importance, however, fibrosis markedly decreased when the sIL-13Rα2-Fc protein was administered, falling to levels that were even lower than those observed in untreated WT mice.

Discussion

Many parasitic helminths induce highly polarized type 2 cytokine responses in their hosts and these responses control a variety of important functional activities including parasite expulsion (17–19), eosinophil activation (57), and development of fibrosis (11, 58). In schistosomiasis, the type 2 cytokine response is primarily directed at the parasite eggs (59) and studies have shown that much of the egg-induced liver pathology is controlled by the relative dominance of type 1 versus type 2 cytokine expression (9, 55). Although it is clear that development of an egg-specific $CD4^+$ Th2-type response is critical for normal granuloma formation (55) and host survival after infection (60, 61), if these responses are too vigorous or persist for too long they can become detrimental and even lethal to the infected host (5, 6). Of the type 2 cytokines examined to date, IL-13 appears to be particularly important because studies show that mice deficient in this cytokine survive longer (12) and fail to develop the fibrotic tissue pathology seen in

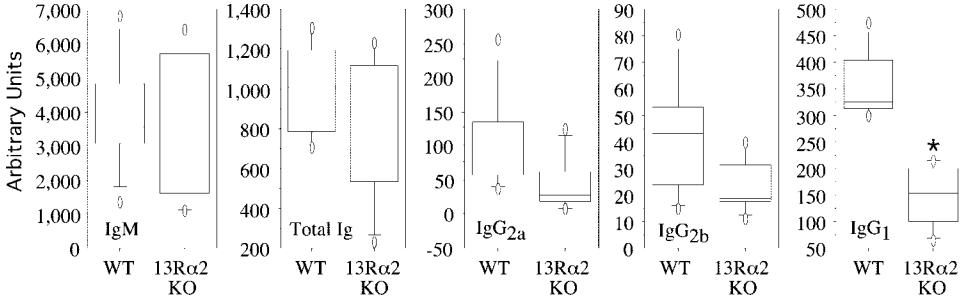

Figure 9. SEA-specific IgG_1 titers decrease in IL-13Rα2–deficient mice. *S. mansoni* egg-specific antibody levels were measured in sera of infected WT and IL-13Rα2–deficient mice (C57BL/6) 9 wk after infection as described in Materials and Methods. Bars from bottom to top show the 10th, 25th, 50th, 75th, and 90th percentiles, respectively, of the tested samples. Single outliners are indicated as circles. Data were obtained from groups of mice containing 6–8 mice/group. *, significant difference when compared with WT values as determined by Student's *t* test. $P < 0.05$. Note that IgG_1 is the predominant egg-specific Ig isotype detected in serum.

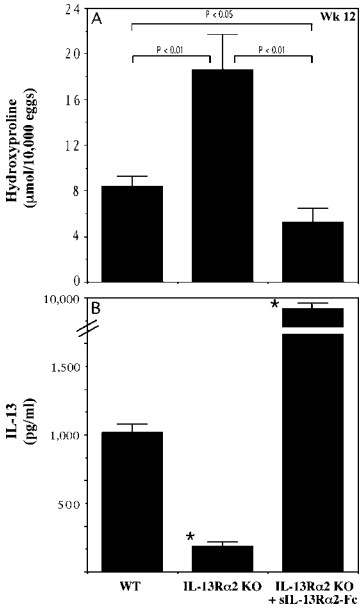

Figure 10. Exacerbated fibrotic response of IL-13Rα2–deficient mice is prevented by administration of sIL-13Rα2-Fc. WT BALB/c and IL-13Rα2–deficient mice were infected with 25–30 cercariae. Beginning on week 6, IL-13Rα2–deficient mice were treated with sIL-13Rα2-Fc or control Ig (200 μg every other day) for a total of 6 wk. All animals were killed on week 12 and fibrosis (A) and serum levels of IL-13 (B) were determined. The values shown are mean values ± SEM for WT ($n = 10$), IL-13Rα2 KO ($n = 10$), and sIL-13Rα2-Fc–treated IL-13Rα2 KO mice ($n = 15$). The P values, as determined by ANOVA, are shown in A. In B: *, significant difference when compared with the WT group as determined by Student's t test. $P < 0.05$.

chronic *S. mansoni* infection (7, 11). Therefore, to better understand disease pathogenesis, it is important to elucidate the mechanisms that control production of IL-13 and/or limit its various effector functions in vivo.

Although IL-4 and IL-13 share many functional activities, we hypothesized that the pathogenic effects of IL-13 are more marked than those of IL-4 because more IL-13 is produced during *S. mansoni* infection (11). Indeed, our studies suggested that IL-13 production is nearly 100-fold greater than IL-4 at the site of granuloma formation. This may in part be explained by the kinetics of the response because IL-4 production is only transiently expressed after egg exposure whereas production of IL-13 is more rapid and sustained over a longer time period (42). Thus, ligand availability is clearly one mechanism regulating the functional activities of these cytokines in vivo. Nevertheless, the pattern of IL-4/IL-13 receptor expression in the liver could be an equally important regulatory mechanism. Before this study, however, there was relatively little known about the IL-4–IL-13 receptor complex and whether expression of the four unique receptor subunits was regulated during infection.

Previous studies showed that IL-13 mRNA expression is induced rapidly after infection, with peak expression occurring in the liver on week 9 and remaining at relatively high levels through 16 wk after infection (7). This work, examining the regulation of the IL-4Rα, γc, IL-13Rα1, and IL-13Rα2 genes, suggests a much more intriguing pattern of expression of the IL-4–IL-13 receptor complex in schistosomiasis. Although the γc and IL-13Rα1 chains showed little evidence of regulation, the signaling IL-4Rα chain and decoy IL-13Rα2 were highly regulated and displayed an opposite pattern of expression in the liver. IL-4Rα mRNA expression was high at early time points and showed little regulation before the onset of egg laying. However, by week 9, ~4 wk after egg laying commences, mRNA levels decreased markedly and remained at low but detectable levels through 16 wk after infection. In contrast, IL-13Rα2 mRNA was almost undetectable at early time points but was up-regulated after egg deposition. In situ hybridization for the three unique IL-4/IL-13–specific receptors showed significant expression of all three receptors throughout the liver of infected mice. IL-13Rα1 was expressed ubiquitously whereas the IL-4Rα chain was found at higher levels within the granuloma and the IL-13Rα2 localized at the periphery. Because IL-13Rα2 followed a pattern that closely mirrored the development of hepatic fibrosis, we examined both the regulation and functional activity of the decoy IL-13 receptor in more detail.

Induction of IL-13Rα2 expression during infection coincides with the emergence of the egg-specific type 2 cytokine response (59). Therefore, we were initially interested in knowing whether type 1 or type 2 cytokines influence receptor up-regulation after infection. Experiments in several cytokine-deficient mice suggested that IL-10 and IL-13 are important mediators of IL-13Rα2 mRNA expression. The effects of IL-10, however, appear to be indirect because mice deficient in both IL-10 and IL-12 showed no reduction in IL-13Rα2 expression. This was in contrast to IL-10 and IL-10/IL-4–deficient mice, which displayed impaired receptor up-regulation. Because IL-10 and IL-10/IL-4–deficient mice develop strong IFN-γ responses, whereas IL-10/IL-12–deficient mice display polarized type 2 cytokine responses (39), these data suggest that IL-10 regulates receptor expression by modulating the dominance of type 1/type 2 cytokine expression. This conclusion was strengthened by our immune deviation studies (Fig. 3 B) in which expression of the decoy receptor was clearly reduced in mice exposed to the Th1-inducing adjuvant IL-12. Moreover, immune deviation studies conducted in IFN-γ–deficient mice suggested that the suppressive effects of IL-12 were largely IFN-γ dependent.

Of even more interest, studies conducted in IL-13–deficient mice demonstrated a critical role for the ligand of the IL-13Rα2 in receptor expression. In contrast to IL-10, these experiments suggest IL-13 acts more directly because exogenous administration of rIL-13 alone rapidly induced IL-13Rα2 mRNA expression in the liver (Fig. 4 B). Levels of IL-13Rα2 also increased in the serum after infection and expression was clearly dependent on IL-4/IL-13 and Stat6-dependent signaling pathways (Fig. 4 C), further emphasizing the importance of type 2 cytokine responses for decoy receptor production. The finding that receptor levels were markedly reduced in IL-13–deficient mice (Fig. 4 A) yet

not significantly altered in IL-4–deficient animals (Fig. 3 A) also suggests IL-13 might be the primary type 2 cytokine stimulating IL-13Rα2 expression. Thus, although it is conceivable that rIL-4 and rIL-13 (Fig. 4 B) would both exhibit IL-13Rα2–inducing activity, IL-13 is likely the more important endogenous inducer simply because it is overproduced relative to IL-4 during infection (11).

In a recent paper examining the regulation of the IL-13Rα2 in human monocytes, Daines and Hershey (62) showed that IL-13Rα2 is rapidly mobilized from intracellular stores to the cell surface after treatment with IFN-γ. The authors hypothesized that induction of IL-13Rα2 expression by IFN-γ might represent a novel mechanism to regulate IL-13 responses. Surprisingly, our data, gathered mostly from in vivo studies, fails to support this hypothesis, which might be explained by the different models being investigated. Alternatively, it may simply indicate that different regulatory mechanisms are exhibited by whole tissues (this study) versus cells stimulated in vitro (62). Our findings demonstrate that the decoy receptor is up-regulated to the greatest extent during polarized Th2 responses. IL-13Rα2 expression was highly IL-13/IL-4–, IL-4R–, and Stat6-dependent. Except for the small twofold decrease observed in the livers of infected IFN-γ–deficient mice, there was no evidence that IFN-γ was required for receptor up-regulation. On the contrary, mice polarized to a Th1-dominant response via treatment with rIL-12 showed decreased IL-13Rα2 expression. This IL-12–induced inhibition of IL-13Rα2 was largely dependent on IFN-γ because in the liver IL-12 failed to reduce receptor expression in IFN-γ KO mice, further highlighting the down-regulatory (rather than up-regulatory) role of IFN-γ in receptor expression. As such, our in vivo data suggest a different regulatory mechanism for the IL-13Rα2 than that proposed by Daines and Hershey (62). Instead of a cross-regulatory system where IFN-γ drives IL-13Rα2 expression to attenuate IL-13 activity, our studies suggest that IL-13Rα2 is a negative feedback mechanism induced by the Th2 response itself. Interestingly, given that this system would act in an antigen-nonspecific way to attenuate IL-13 activity, this mechanism of helminth-induced IL-13Rα2 expression could, at least in part, also provide an explanation for the hygiene hypothesis, which suggests that the increase in allergic disease observed in westernized countries is due to decreased exposure to childhood infections (63). Our findings demonstrate that schistosome infection provides a potent stimulus for decoy receptor expression, which presumably could act as a bystander mechanism to neutralize the allergy-inducing potential of IL-13.

Although expression of the IL-13Rα2 correlated with development of fibrosis (Fig. 2 B), the role of the endogenous IL-13Rα2 remained hypothetical until KO studies could be conducted. In previous work, we showed that administration of sIL-13Rα2-Fc fusion protein was highly efficacious for the prevention of fibrotic liver pathology (11). Moreover, recent studies demonstrated that IL-13 antagonism could also be used to block the progression of established disease (7). As such, these findings suggest that a primary function of the IL-13Rα2 is to inhibit the profibrotic activity of IL-13. To directly test this hypothesis and evaluate the function of the endogenous IL-13Rα2, we infected mice with a targeted deletion of IL-13Rα2 (38). Strikingly, hepatic fibrosis increased significantly in IL-13Rα2–deficient mice. Importantly, these data were reproducible in KO mice generated on two different genetic backgrounds, providing one of the first in vivo examples of functional decoy activity for the endogenous IL-13Rα2.

The pattern of liver fibrosis in the IL-13Rα2–deficient animals was also quite intriguing. Although fibrosis in WT mice was primarily restricted to the areas surrounding the developing granulomas, collagen staining in the KO mice extended beyond the areas of lesion formation and appeared to spread throughout the liver parenchyma itself. These data suggest that the protective function of the decoy receptor might extend to areas not directly affected by the parasite eggs. Nevertheless, the exacerbated fibrotic response appeared to be restricted to the liver because hydroxyproline assays performed on kidney, lung, and brain of infected IL-13Rα2–deficient mice showed no evidence of excess collagen deposition in these nongranulomatous tissues (unpublished data). These findings are important because nanogram quantities of IL-13 are detectable in the serum of infected mice (Fig. 10 B) and the absence of decoy receptor could trigger fibrogenesis in tissues not directly affected by the parasite eggs. In some *S. mansoni*–infected humans, pipe stem fibrosis along the hepatic portal tracks is not necessarily associated with the egg-induced granulomas (64). It is intriguing to speculate that if the IL-13Rα2 exhibits similar protective activity in humans, it might represent an important mechanism to prevent fibrosis at distant sites within the liver.

Markedly, the increase in hepatic fibrosis in IL-13Rα2–deficient mice on week 9 was not accompanied by any obvious change in the size nor cellular composition of the granulomas. Similar findings were also reported in infected IL-13Rα2-Fc–treated (11) and IL-13–deficient mice (12). In each of these studies, granulomatous inflammation was regulated by the combined actions of IL-4 and IL-13 whereas fibrosis was regulated primarily by IL-13. Thus, the primary function of IL-13 and its receptors appears to be the regulation of fibrosis. Hepatic fibrosis in schistosomiasis is also tightly controlled by the relative dominance of IFN-γ versus IL-13 produced locally in the liver (7). Indeed, studies showed that mice that produce high levels of IL-13 and low levels of IFN-γ develop much more severe fibrosis than animals that have a high IFN-γ/IL-13 ratio (5, 65). Therefore, we were interested in knowing whether changes in type 1/type 2 cytokine dominance were contributing to the exacerbated fibrotic response. Strikingly, however, our findings suggested that type 2 cytokine expression was actually decreasing in the livers of the KO animals (Fig. 8). This conclusion was strengthened by analyzing serum levels of IL-13, which were also markedly reduced in the IL-13Rα2–deficient mice (Fig. 10). Finally, decreasing levels of egg-specific IgG1 Abs (the dominant Ab isotype expressed during infection) provided additional

evidence of a general decline in type 2 cytokine expression (Fig. 9). Thus, fibrosis increases in the IL-13Rα2 KO mice despite the significant decrease in IL-13 levels. Importantly, expression of IL-13Rα1 and IL-4Rα mRNA chains did not differ in the WT and IL-13Rα2–deficient mice, which may explain why IL-13 remains active in both animals. These results suggest that even reduced levels of IL-13 are sufficient to generate significant fibrosis when IL-13Rα2 expression is low or absent. As such, these findings add additional weight to the importance of the IL-13Rα2 in the regulation of type 2 immune responses because they clearly demonstrate an enhancement of IL-13 activity in the absence of the decoy receptor. The results also suggest the decoy receptor has a much greater influence on the development of fibrosis than the relative level of IL-13.

The decrease in IL-13 expression in the KO mice was particularly surprising because it is clear from both blocking and KO studies that IL-13 is required for the development of hepatic fibrosis in schistosomiasis (11, 12). These findings suggest that a sensitive and highly regulated mechanism is in place to control production of IL-13, IL-13Rα2, and development of tissue fibrosis. This elegant system for controlling tissue pathology was best exemplified in the last series of experiments (Fig. 10) in which IL-13Rα2 activity was restored in the KO mice by treating them with a sIL-13Rα2-Fc construct. Fibrosis more than doubled by 12 wk after infection in the IL-13Rα2–deficient mice whereas the fibrotic response was largely prevented in the group receiving sIL-13Rα2-Fc. In fact, the sIL-13Rα2-Fc construct reduced fibrosis in the KO animals by >70%, formally demonstrating that their exacerbated pattern of fibrosis was entirely due to the absence of IL-13Rα2 expression and heightened IL-13 activity. We observed that the impaired serum IL-13 response in the KO animals was restored and even increased after administration of sIL-13Rα2-Fc (Fig. 10). As such, these data suggest that as fibrosis increases in IL-13Rα2–deficient mice, IL-13 levels drop, perhaps to compensate for the worsening tissue response. Similarly, when fibrosis is reduced in the KO mice after sIL-13Rα-Fc treatment, levels of the profibrotic cytokine IL-13 increase in the serum. Alternatively, IL-13 may simply act as a negative regulator of its own production. It is also possible that serum levels of IL-13 increase after sIL-13Rα2-Fc treatment because the receptor is acting as a depot or carrier for the cytokine, essentially extending the in vivo half-life of IL-13 via a mechanism analogous to cytokine–anti–cytokine antibody complexes (38, 66). Regardless of the exact mechanisms involved, this reciprocal pattern of regulation suggests that a tight balance between IL-13 and IL-13Rα2 expression might be required for the establishment of an optimal healing response.

Th2-mediated inflammation plays a central role in the pathogenesis of a variety of other fibrotic disorders including asthma (29), idiopathic pulmonary fibrosis (67, 68), chronic graft rejection (69), bleomycin-induced pulmonary fibrosis (70), progressive systemic sclerosis (71), radiation-induced pulmonary fibrosis (72), and hepatic fibrosis (9, 11, 12, 73). The studies presented here document the important protective function of the endogenous IL-13Rα2 and its role in the inhibition of IL-13–mediated tissue fibrosis. Moreover, these studies demonstrate that the decoy IL-13Rα2 can also regulate the magnitude of Th2-type cytokine production in vivo. As such, our findings illustrate a novel and previously unappreciated mechanism for limiting the pathogenesis of chronic Th2-mediated inflammatory responses.

The authors thank Karl Hoffmann and Matthias Hesse for providing reagents and excellent advice, Netanya Sandler and Mary Leusink for comments and suggestions on the manuscript, Andrew McKenzie for breeding pairs of IL-13–deficient mice, Fred Lewis (Biomedical Research Institute) for providing parasite materials, and Rick Dreyfuss for help with the photomicrographs.

M.J. Grusby is a Scholar of the Leukemia and Lymphoma Society of America and supported by NIH grant AI4040171, a grant from the Sandler Program for Asthma Research, and the Mathers Foundation.

Submitted: 4 June 2002
Revised: 20 January 2003
Accepted: 22 January 2003

References

1. Opal, S.M., and V.A. DePalo. 2000. Anti-inflammatory cytokines. *Chest.* 117:1162–1172.
2. Finkelman, F.D., T.A. Wynn, D.D. Donaldson, and J.F. Urban. 1999. The role of IL-13 in helminth-induced inflammation and protective immunity against nematode infections. *Curr. Opin. Immunol.* 11:420–426.
3. Gazzinelli, R.T., M. Wysocka, S. Hieny, T. Scharton-Kersten, A. Cheever, R. Kuhn, W. Muller, G. Trinchieri, and A. Sher. 1996. In the absence of endogenous IL-10, mice acutely infected with Toxoplasma gondii succumb to a lethal immune response dependent on CD4+ T cells and accompanied by overproduction of IL-12, IFN-gamma and TNF-alpha. *J. Immunol.* 157:798–805.
4. Hunter, C.A., L.A. Ellis-Neyes, T. Slifer, S. Kanaly, G. Grunig, M. Fort, D. Rennick, and F.G. Araujo. 1997. IL-10 is required to prevent immune hyperactivity during infection with Trypanosoma cruzi. *J. Immunol.* 158:3311–3316.
5. Hoffmann, K.F., A.W. Cheever, and T.A. Wynn. 2000. IL-10 and the dangers of immune polarization: excessive type 1 and type 2 cytokine responses induce distinct forms of lethal immunopathology in murine schistosomiasis. *J. Immunol.* 164:6406–6416.
6. Hoffmann, K.F., T.C. McCarty, D.H. Segal, M. Chiaramonte, M. Hesse, E.M. Davis, A.W. Cheever, P.S. Meltzer, H.C. Morse III, and T.A. Wynn. 2001. Disease fingerprinting with cDNA microarrays reveals distinct gene expression profiles in lethal type 1 and type 2 cytokine-mediated inflammatory reactions. *FASEB J.* 15:2545–2547.
7. Chiaramonte, M.G., A.W. Cheever, J.D. Malley, D.D. Donaldson, and T.A. Wynn. 2001. Studies of murine schistosomiasis reveal interleukin-13 blockade as a treatment for established and progressive liver fibrosis. *Hepatology.* 34:273–282.
8. Wynn, T.A., and A.W. Cheever. 1995. Cytokine regulation of granuloma formation in schistosomiasis. *Curr. Opin. Immunol.* 7:505–511.
9. Wynn, T.A., A.W. Cheever, D. Jankovic, R.W. Poindexter,

P. Caspar, F.A. Lewis, and A. Sher. 1995. An IL-12-based vaccination method for preventing fibrosis induced by schistosome infection. *Nature*. 376:594–596.

10. Cheever, A.W., M.E. Williams, T.A. Wynn, F.D. Finkelman, R.A. Seder, T.M. Cox, S. Hieny, P. Caspar, and A. Sher. 1994. Anti-IL-4 treatment of Schistosoma mansoni-infected mice inhibits development of T cells and non-B, non-T cells expressing Th2 cytokines while decreasing egg-induced hepatic fibrosis. *J. Immunol.* 153:753–759.
11. Chiaramonte, M.G., D.D. Donaldson, A.W. Cheever, and T.A. Wynn. 1999. An IL-13 inhibitor blocks the development of hepatic fibrosis during a T-helper type 2-dominated inflammatory response. *J. Clin. Invest.* 104:777–785.
12. Fallon, P.G., E.J. Richardson, G.J. McKenzie, and A.N. McKenzie. 2000. Schistosome infection of transgenic mice defines distinct and contrasting pathogenic roles for IL-4 and IL-13: IL-13 is a profibrotic agent. *J. Immunol.* 164:2585–2591.
13. Pearce, E.J., A. Cheever, S. Leonard, M. Covalesky, R. Fernandez-Botran, G. Kohler, and M. Kopf. 1996. Schistosoma mansoni in IL-4-deficient mice. *Int. Immunol.* 8:435–444.
14. Jankovic, D., M.C. Kullberg, N. Noben-Trauth, P. Caspar, J.M. Ward, A.W. Cheever, W.E. Paul, and A. Sher. 1999. Schistosome-infected IL-4 receptor knockout (KO) mice, in contrast to IL-4 KO mice, fail to develop granulomatous pathology while maintaining the same lymphokine expression profile. *J. Immunol.* 163:337–342.
15. Wynn, T.A., R. Morawetz, T. Scharton-Kersten, S. Hieny, H.C. Morse, R. Kuhn, W. Muller, A.W. Cheever, and A. Sher. 1997. Analysis of granuloma formation in double cytokine-deficient mice reveals a central role for IL-10 in polarizing both T helper cell 1- and T helper cell 2-type cytokine responses in vivo. *J. Immunol.* 159:5014–5023.
16. Cheever, A.W. 1972. Pipe-stem fibrosis of the liver. *Trans. R. Soc. Trop. Med. Hyg.* 66:947–948.
17. McKenzie, G.J., A. Bancroft, R.K. Grencis, and A.N. McKenzie. 1998. A distinct role for interleukin-13 in Th2-cell-mediated immune responses. *Curr. Biol.* 8:339–342.
18. Bancroft, A.J., A.N. McKenzie, and R.K. Grencis. 1998. A critical role for IL-13 in resistance to intestinal nematode infection. *J. Immunol.* 160:3453–3461.
19. Urban, J.F., Jr., N. Noben-Trauth, D.D. Donaldson, K.B. Madden, S.C. Morris, M. Collins, and F.D. Finkelman. 1998. IL-13, IL-4Ralpha, and Stat6 are required for the expulsion of the gastrointestinal nematode parasite Nippostrongylus brasiliensis. *Immunity.* 8:255–264.
20. Terabe, M., S. Matsui, N. Noben-Trauth, H. Chen, C. Watson, D.D. Donaldson, D.P. Carbone, W.E. Paul, and J.A. Berzofsky. 2000. NKT cell-mediated repression of tumor immunosurveillance by IL-13 and the IL-4R-STAT6 pathway. *Nat. Immunol.* 1:515–520.
21. Zhu, Z., R.J. Homer, Z. Wang, Q. Chen, G.P. Geba, J. Wang, Y. Zhang, and J.A. Elias. 1999. Pulmonary expression of interleukin-13 causes inflammation, mucus hypersecretion, subepithelial fibrosis, physiologic abnormalities, and eotaxin production. *J. Clin. Invest.* 103:779–788.
22. Wills-Karp, M., J. Luyimbazi, X. Xu, B. Schofield, T.Y. Neben, C.L. Karp, and D.D. Donaldson. 1998. Interleukin-13: central mediator of allergic asthma. *Science.* 282:2258–2261.
23. Grunig, G., M. Warnock, A.E. Wakil, R. Venkayya, F. Brombacher, D.M. Rennick, D. Sheppard, M. Mohrs, D.D. Donaldson, R.M. Locksley, et al. 1998. Requirement for IL-13 independently of IL-4 in experimental asthma. *Science.* 282:2261–2263.
24. Russell, S.M., A.D. Keegan, N. Harada, Y. Nakamura, M. Noguchi, P. Leland, M.C. Friedmann, A. Miyajima, R.K. Puri, W.E. Paul, et al. 1993. Interleukin-2 receptor gamma chain: a functional component of the interleukin-4 receptor. *Science.* 262:1880–1883.
25. Hilton, D.J., J.G. Zhang, D. Metcalf, W.S. Alexander, N.A. Nicola, and T.A. Willson. 1996. Cloning and characterization of a binding subunit of the interleukin 13 receptor that is also a component of the interleukin 4 receptor. *Proc. Natl. Acad. Sci. USA.* 93:497–501.
26. Miloux, B., P. Laurent, O. Bonnin, J. Lupker, D. Caput, N. Vita, and P. Ferrara. 1997. Cloning of the human IL-13R alpha1 chain and reconstitution with the IL4R alpha of a functional IL-4/IL-13 receptor complex. *FEBS Lett.* 401: 163–166.
27. Nelms, K., A.D. Keegan, J. Zamorano, J.J. Ryan, and W.E. Paul. 1999. The IL-4 receptor: signaling mechanisms and biologic functions. *Annu. Rev. Immunol.* 17:701–738.
28. Caput, D., P. Laurent, M. Kaghad, J.M. Lelias, S. Lefort, N. Vita, and P. Ferrara. 1996. Cloning and characterization of a specific interleukin (IL)-13 binding protein structurally related to the IL-5 receptor alpha chain. *J. Biol. Chem.* 271: 16921–16926.
29. Donaldson, D.D., M.J. Whitters, L.J. Fitz, T.Y. Neben, H. Finnerty, S.L. Henderson, R.M. O'Hara, Jr., D.R. Beier, K.J. Turner, C.R. Wood, et al. 1998. The murine IL-13 receptor alpha 2: molecular cloning, characterization, and comparison with murine IL-13 receptor alpha 1. *J. Immunol.* 161: 2317–2324.
30. Kawakami, K., J. Taguchi, T. Murata, and R.K. Puri. 2001. The interleukin-13 receptor alpha2 chain: an essential component for binding and internalization but not for interleukin-13-induced signal transduction through the STAT6 pathway. *Blood.* 97:2673–2679.
31. Murata, T., N.I. Obiri, and R.K. Puri. 1998. Structure of and signal transduction through interleukin-4 and interleukin-13 receptors. *Int. J. Mol. Med.* 1:551–557.
32. Bernard, J., D. Treton, C. Vermot-Desroches, C. Boden, P. Horellou, E. Angevin, P. Galanaud, J. Wijdenes, and Y. Richard. 2001. Expression of interleukin 13 receptor in glioma and renal cell carcinoma: IL13Ralpha2 as a decoy receptor for IL13. *Lab. Invest.* 81:1223–1231.
33. Feng, N., S.M. Lugli, B. Schnyder, J.F. Gauchat, P. Graber, E. Schlagenhauf, B. Schnarr, M. Wiederkehr-Adam, A. Duschl, M.H. Heim, et al. 1998. The interleukin-4/interleukin-13 receptor of human synovial fibroblasts: overexpression of the nonsignaling interleukin-13 receptor alpha2. *Lab. Invest.* 78:591–602.
34. Colotta, F., F. Re, M. Muzio, R. Bertini, N. Polentarutti, M. Sironi, J.G. Giri, S.K. Dower, J.E. Sims, and A. Mantovani. 1993. Interleukin-1 type II receptor: a decoy target for IL-1 that is regulated by IL-4. *Science.* 261:472–475.
35. Morse, B., J.P. Sypek, D.D. Donaldson, K.J. Haley, and C.M. Lilly. 2002. Effects of IL-13 on airway responses in the guinea pig. *Am. J. Physiol. Lung Cell. Mol. Physiol.* 282:L44–L49.
36. Walter, D.M., J.J. McIntire, G. Berry, A.N. McKenzie, D.D. Donaldson, R.H. DeKruyff, and D.T. Umetsu. 2001. Critical role for IL-13 in the development of allergen-induced airway hyperreactivity. *J. Immunol.* 167:4668–4675.

37. Urban, J., H. Fang, Q. Liu, M.J. Ekkens, S.J. Chen, D. Nguyen, V. Mitro, D.D. Donaldson, C. Byrd, R. Peach, et al. 2000. IL-13-mediated worm expulsion is B7 independent and IFN-gamma sensitive. *J. Immunol.* 164:4250–4256.
38. Wood, N., M. Whitters, B.A. Jacobson, J. Witek, J.P. Sypek, M. Kasaian, M. Eppihimer, M. Unger, S. Goldman, M. Collins, et al. 2003. Enhanced IL-13 responses in mice lacking IL-13Rα. *J. Exp. Med.* 197:703–709.
39. Hoffmann, K.F., S.L. James, A.W. Cheever, and T.A. Wynn. 1999. Studies with double cytokine-deficient mice reveal that highly polarized Th1- and Th2-type cytokine and antibody responses contribute equally to vaccine-induced immunity to *Schistosoma mansoni*. *J. Immunol.* 163:927–938.
40. Kaplan, M.H., U. Schindler, S.T. Smiley, and M.J. Grusby. 1996. Stat6 is required for mediating responses to IL-4 and for development of Th2 cells. *Immunity.* 4:313–319.
41. Hesse, M., A.W. Cheever, D. Jankovic, and T.A. Wynn. 2000. NOS-2 mediates the protective anti-inflammatory and antifibrotic effects of the Th1-inducing adjuvant, IL-12, in a Th2 model of granulomatous disease. *Am. J. Pathol.* 157:945–955.
42. Chiaramonte, M.G., L.R. Schopf, T.Y. Neben, A.W. Cheever, D.D. Donaldson, and T.A. Wynn. 1999. IL-13 is a key regulatory cytokine for Th2 cell-mediated pulmonary granuloma formation and IgE responses induced by Schistosoma mansoni eggs. *J. Immunol.* 162:920–930.
43. Bergman, I., and R. Loxley. 1963. Two improved and simplified methods for the spectrophotometric determination of hydroxyproline. *Anal. Biochem.* 35:1961–1965.
44. Wynn, T.A., I. Eltoum, A.W. Cheever, F.A. Lewis, W.C. Gause, and A. Sher. 1993. Analysis of cytokine mRNA expression during primary granuloma formation induced by eggs of *Schistosoma mansoni*. *J. Immunol.* 151:1430–1440.
45. Finkelman, F.D., and S.C. Morris. 1999. Development of an assay to measure in vivo cytokine production in the mouse. *Int. Immunol.* 11:1811–1818.
46. Cheever, A.W., R.H. Duvall, T.A. Hallack, Jr., R.G. Minker, J.D. Malley, and K.G. Malley. 1987. Variation of hepatic fibrosis and granuloma size among mouse strains infected with Schistosoma mansoni. *Am. J. Trop. Med. Hyg.* 37: 85–97.
47. Wynn, T.A., I. Eltoum, I.P. Oswald, A.W. Cheever, and A. Sher. 1994. Endogenous interleukin 12 (IL-12) regulates granuloma formation induced by eggs of *Schistosoma mansoni* and exogenous IL-12 both inhibits and prophylactically immunizes against egg pathology. *J. Exp. Med.* 179:1551–1561.
48. Zhang, J.G., D.J. Hilton, T.A. Willson, C. McFarlane, B.A. Roberts, R.L. Moritz, R.J. Simpson, W.S. Alexander, D. Metcalf, and N.A. Nicola. 1997. Identification, purification, and characterization of a soluble interleukin (IL)-13-binding protein. Evidence that it is distinct from the cloned Il-13 receptor and Il-4 receptor alpha-chains. *J. Biol. Chem.* 272: 9474–9480.
49. Amiri, P., R.M. Locksley, T.G. Parslow, M. Sadick, E. Rector, D. Ritter, and J.H. McKerrow. 1992. Tumour necrosis factor alpha restores granulomas and induces parasite egg-laying in schistosome-infected SCID mice. *Nature.* 356:604–607.
50. Wolowczuk, I., S. Nutten, O. Roye, M. Delacre, M. Capron, R.M. Murray, F. Trottein, and C. Auriault. 1999. Infection of mice lacking interleukin-7 (IL-7) reveals an unexpected role for IL-7 in the development of the parasite Schistosoma mansoni. *Infect. Immun.* 67:4183–4190.
51. Lanone, S., T. Zheng, Z. Zhu, W. Liu, C.G. Lee, B. Ma, Q. Chen, R.J. Homer, J. Wang, L.A. Rabach, et al. 2002. Overlapping and enzyme-specific contributions of matrix metalloproteinases-9 and -12 in IL-13-induced inflammation and remodeling. *J. Clin. Invest.* 110:463–474.
52. Reeves, H.L., and S.L. Friedman. 2002. Activation of hepatic stellate cells–a key issue in liver fibrosis. *Front. Biosci.* 7:d808–d826.
53. Hesse, M., M. Modolell, A.C. La Flamme, M. Schito, J.M. Fuentes, A.W. Cheever, E.J. Pearce, and T.A. Wynn. 2001. Differential regulation of nitric oxide synthase-2 and arginase-1 by type 1/type 2 cytokines in vivo: granulomatous pathology is shaped by the pattern of L-arginine metabolism. *J. Immunol.* 167:6533–6544.
54. Modolell, M., I.M. Corraliza, F. Link, G. Soler, and K. Eichmann. 1995. Reciprocal regulation of the nitric oxide synthase/arginase balance in mouse bone marrow-derived macrophages by TH1 and TH2 cytokines. *Eur. J. Immunol.* 25: 1101–1104.
55. Kaplan, M.H., J.R. Whitfield, D.L. Boros, and M.J. Grusby. 1998. Th2 cells are required for the *Schistosoma mansoni* egg-induced granulomatous response. *J. Immunol.* 160:1850–1856.
56. Fulton, R.J., R.L. McDade, P.L. Smith, L.J. Kienker, and J.R. Kettman, Jr. 1997. Advanced multiplexed analysis with the FlowMetrix system. *Clin. Chem.* 43:1749–1756.
57. Lopez, A.F., C.J. Sanderson, J.R. Gamble, H.D. Campbell, I.G. Young, and M.A. Vadas. 1988. Recombinant human interleukin 5 is a selective activator of human eosinophil function. *J. Exp. Med.* 167:219–224.
58. Lee, C.G., R.J. Homer, Z. Zhu, S. Lanone, X. Wang, V. Koteliansky, J.M. Shipley, P. Gotwals, P. Noble, Q. Chen, et al. 2001. Interleukin-13 induces tissue fibrosis by selectively stimulating and activating transforming growth factor β(1). *J. Exp. Med.* 194:809–821.
59. Grzych, J.M., E.J. Pearce, A. Cheever, Z.A. Caulada, P. Caspar, S. Heiny, F. Lewis, and A. Sher. 1991. Egg deposition is the major stimulus for the production of Th2 cytokines in murine schistosomiasis mansoni. *J. Immunol.* 146:1322–1327.
60. Brunet, L.R., F.D. Finkelman, A.W. Cheever, M.A. Kopf, and E.J. Pearce. 1997. IL-4 protects against TNF-alpha-mediated cachexia and death during acute schistosomiasis. *J. Immunol.* 159:777–785.
61. Fallon, P.G., E.J. Richardson, P. Smith, and D.W. Dunne. 2000. Elevated type 1, diminished type 2 cytokines and impaired antibody response are associated with hepatotoxicity and mortalities during Schistosoma mansoni infection of CD4-depleted mice. *Eur. J. Immunol.* 30:470–480.
62. Daines, M.O., and G.K. Hershey. 2002. A novel mechanism by which interferon-gamma can regulate interleukin (IL)-13 responses. Evidence for intracellular stores of IL-13 receptor alpha-2 and their rapid mobilization by interferon-gamma. *J. Biol. Chem.* 277:10387–10393.
63. Wills-Karp, M., J. Santeliz, and C.L. Karp. 2001. The germless theory of allergic disease: revisiting the hygiene hypothesis. *Nat. Rev. Immunol.* 1:69–75.
64. Von Lichtenberg, F., and E.H. Sadun. 1968. Experimental production of bilharzial pipe-stem fibrosis in the chimpanzee. *Exp. Parasitol.* 22:264–278.
65. Vaillant, B., M.G. Chiaramonte, A.W. Cheever, P.D. Soloway, and T.A. Wynn. 2001. Regulation of hepatic fibrosis and extracellular matrix genes by the Th response: new insight into the role of tissue inhibitors of matrix metallopro-

teinases. *J. Immunol.* 167:7017–7026.
66. Finkelman, F.D., K.B. Madden, S.C. Morris, J.M. Holmes, N. Boiani, I.M. Katona, and C.R. Maliszewski. 1993. Anti-cytokine antibodies as carrier proteins. Prolongation of in vivo effects of exogenous cytokines by injection of cytokine-anti-cytokine antibody complexes. *J. Immunol.* 151:1235–1244.
67. Majumdar, S., D. Li, T. Ansari, P. Pantelidis, C.M. Black, M. Gizycki, R.M. du Bois, and P.K. Jeffery. 1999. Different cytokine profiles in cryptogenic fibrosing alveolitis and fibrosing alveolitis associated with systemic sclerosis: a quantitative study of open lung biopsies. *Eur. Respir. J.* 14:251–257.
68. Wallace, W.A., E.A. Ramage, D. Lamb, and S.E. Howie. 1995. A type 2 (Th2-like) pattern of immune response predominates in the pulmonary interstitium of patients with cryptogenic fibrosing alveolitis (CFA). *Clin. Exp. Immunol.* 101:436–441.
69. Shirwan, H. 1999. Chronic allograft rejection. Do the Th2 cells preferentially induced by indirect alloantigen recognition play a dominant role? *Transplantation.* 68:715–726.
70. Baecher-Allan, C.M., and R.K. Barth. 1993. PCR analysis of cytokine induction profiles associated with mouse strain variation in susceptibility to pulmonary fibrosis. *Reg. Immunol.* 5:207–217.
71. Hasegawa, M., M. Fujimoto, K. Kikuchi, and K. Takehara. 1997. Elevated serum levels of interleukin 4 (IL-4), IL-10, and IL-13 in patients with systemic sclerosis. *J. Rheumatol.* 24: 328–332.
72. Westermann, W., R. Schobl, E.P. Rieber, and K.H. Frank. 1999. Th2 cells as effectors in postirradiation pulmonary damage preceding fibrosis in the rat. *Int. J. Radiat. Biol.* 75: 629–638.
73. Shi, Z., A.E. Wakil, and D.C. Rockey. 1997. Strain-specific differences in mouse hepatic wound healing are mediated by divergent T helper cytokine responses. *Proc. Natl. Acad. Sci. USA.* 94:10663–10668.